

Vesicles, amygdales and similar structures in fault-generated pseudotachylytes

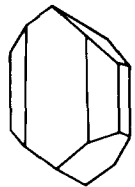
R.H. MADDOCK¹*, J. GROCOTT² and M. VAN NES³

¹Department of Geology, Royal School of Mines, Imperial College, London SW7 2BP (Great Britain)

²School of Geological Sciences, Kingston Polytechnic, Penrhyn Road, Kingston-upon-Thames KT1 2EE (Great Britain)

³Instituut voor Aardwetenschappen, Budapestlaan 4, 3508 TA Utrecht (The Netherlands)

LITHOS



Maddock, R.H., Grocott, J. and Van Nes, M., 1987. Vesicles, amygdales and similar structures in fault-generated pseudotachylytes. *Lithos*, 20: 419–432.

Amygdales in fault-generated pseudotachylytes from the Outer Hebrides Thrust, Scotland, and the Iker-tôq Shear Belt, West Greenland, contain mineral assemblages dominated by K-spar + sphene + epidote + quartz and carbonates respectively. These contrasting assemblages indicate that vesicle infilling took place under differing environmental conditions. Other 'filled cavities', resembling amygdales in form and mineralogy, are recognized as replacement pseudomorphs after porphyroclasts. Using published data relating vesicle abundance and solubility functions for H₂O and CO₂ to pressure, a palaeoseismic depth estimate (equivalent to the depth of vesiculation) of about 1.6 km is inferred for the Greenland pseudotachylytes described in this paper.

(Received January 16, 1986; accepted August 21, 1986)

Introduction

Fault-generated pseudotachylytes (hereafter simply termed pseudotachylytes) are believed to form by frictional melting during earthquake faulting, predominantly in cold dry crystalline rocks (McKenzie and Brune, 1972; Sibson, 1975), although an essentially cataclastic origin has also been proposed (Wenk, 1978). They form at depths ranging from perhaps in excess of 15 km, where the dominant mode of deformation is plastic (e.g. Sibson, 1980; Passchier, 1982), to as little as 0.5 km – for example along the Alpine Fault zone, New Zealand (R.H. Sibson, pers. commun., 1982). Pseudotachylytes which can be shown unequivocally to have cooled from a melt (e.g. Philpotts, 1964; Maddock, 1983, 1986a; Macaudière et al., 1985) occasionally contain amygdales, permitting refinement of estimates of depth of generation, i.e. palaeoseismic depths according to the model of Sibson

(1975). A second type of structure resembling a filled cavity, results from in situ alteration and replacement of porphyroclasts, forming pseudomorphs which may superficially resemble amygdales. The purpose of this contribution is to describe the form and mineralogy of these structures and attempt to deduce certain environmental conditions (temperature, fluid composition and especially confining pressure) during and after pseudotachylyte generation.

Method of study

Polished thin sections of pseudotachylyte were examined optically and by scanning electron microscopy (SEM) operating in the backscattered electron (BSE) mode, which is ideal for studying fine-grained and mineralogically heterogeneous rocks (cf. Hall and Lloyd, 1981). Quantitative and semi-quantitative mineral analyses were obtained in a JEOL 733 SEM and a Cambridge Instruments Microscan V electron microprobe, both fitted with

*Present address: 31, Mapesbury Road, London, NW2 4HS, U.K.

Link Systems energy-dispersive X-ray analysers. Both instruments were operated at 15 kV excitation voltage and a beam current of 80–120 μ A; well-characterized mineral standards were analyzed at the same time as the samples.

Sample localities

The pseudotachylytes of this study were collected from the Outer Hebrides Thrust (OHT), NW Scotland and the Ikertôq Shear Belt, West Greenland. Both of these major fault zones have a long history of deformation and contain abundant pseudotachylyte, cataclasite and mylonite series faultrocks (terminology of Sibson, 1977a).

The OHT cuts Lewisian Gneisses and the pseudotachylyte faulting probably occurred during Caledonian times (Sibson, 1977a); the main thrust was subsequently reactivated as a major extensional fault (Smythe et al., 1982). A suite of amygdaloidal pseudotachylytes were collected from a sub-vertical quasiconglomerate vein complex (see Sibson, 1975; Grocott, 1981, for terminology) cutting amphibolite facies quartzofeldspathic gneiss at Rubha Ardvule, South Uist (Grid reference NF7130), some 8 km W of the main thrust base. The NW-trending, sub-vertical pseudotachylytes at this locality antedate gently E-dipping vein systems (Maddock, 1986b). Amygdaloidal pseudotachylytes have not previously been reported from the

OHT, their absence having been used to infer a minimum depth of generation of 2 km (cf. Sibson, 1975).

The Ikertôq Shear Belt is a major shear zone in which the main displacements occurred in the period 2700–1650 Ma, when the gneisses in the belt were reworked under amphibolite and granulite facies conditions (Bak et al., 1975; Grocott, 1979). Since then the shear belt has been reactivated several times (Watterson, 1975). In the N part of the belt, where material for this study was collected, palaeomagnetic data from seven sites point to a late Proterozoic reactivation of the belt, either at ca. 1220 Ma or at ca. 600 Ma (Piper, 1981a). Unfortunately the palaeomagnetic data cannot discriminate between these results, and although Piper (1981a) believes the latter age to be that of pseudotachylyte formation, his arguments are equivocal.

The gneisses of the shear belt are cut by a suite of kimberlite and lamproite dykes (B.H. Scott, 1981). Field relationships between faults on which pseudotachylyte was generated and certain lamproite dykes in the northern part of the shear belt clearly show that faulting and dyke intrusion were contemporaneous. The dykes occupy extensional fractures for the most part, but they change trend and intrusion geometry as they approach pseudotachylyte generation zones in which they occupy extensional shear fractures. Further evidence of contemporaneity exists where dykes having identical petrology and field appearance can be shown to have intruded sin-

TABLE 1
Mineralogy of amygdales in Outer Hebrides pseudotachylyte

| Phase | Composition (determined by electron microprobe) | Zonation/occurrence |
|------------------------|--------------------------------------------------------------------------------------------------------------------------------------------|-----------------------|
| K-spar | $Or_{95.37}Ab_{4.19}An_{0.44}$ | } "essential" phases |
| Quartz | | |
| Sphene Epidote 1 | $Ca_{4.05}(Ti_{3.64}Fe_{0.14}^{3+}Al_{0.29})Si_{4.00}O_{20}$ | |
| Epidote 2 | $(Ca_{1.94}Na_{0.11}K_{0.01})(Mg_{3.28}Fe_{1.58}^{2+}Fe_{0.06}^{3+}Mn_{0.07}Ti_{0.04}Al_{0.04}^{IV})(Si_{7.78}Al_{0.22}^{IV})O_{22}(OH)_2$ | } "accessory" phases |
| Actinolite | $(K_{1.57}Ca_{0.03})(Fe_{2.24}Mg_{3.11}Mn_{0.04}Ti_{0.28}Al_{0.29}^{IV})(Si_{5.63}Al_{2.37}^{IV})O_{20}(OH)_4$ | |
| Biotite | | |
| Apatite | | |
| Magnetite | | |
| Pyrite Chalcopyrite | | |
| Chlorite | $(K_{0.68}Ca_{0.06})(Mg_{4.78}Fe_{3.20}Mn_{0.06}Ti_{0.21}Al_{2.50}^{IV})(Si_{6.68}Al_{1.14}^{IV})O_{20}(OH)_{16}$ | } "alteration" phases |
| Fe-hydroxide | | |
| Albite | $Or_{0.61}Ab_{98.64}An_{0.76}$ (with K-spar) | microjoints |

PLATE I

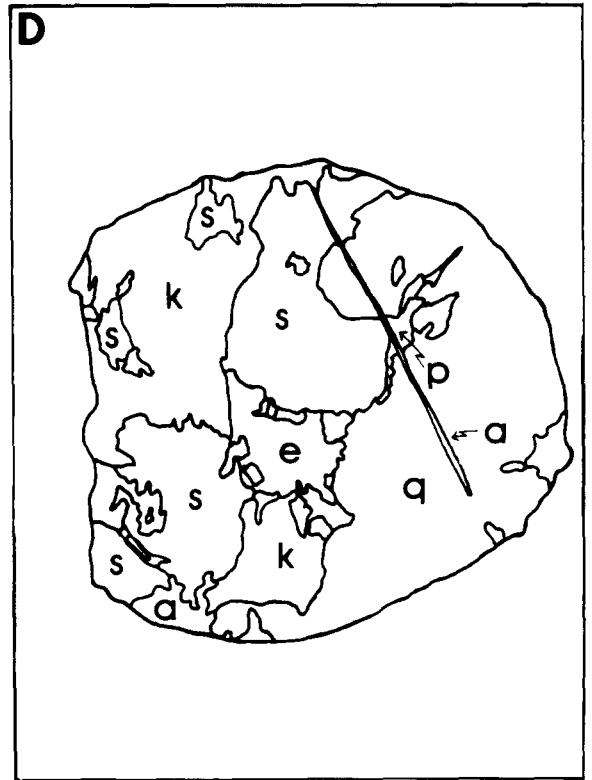


PLATE I (continued)



gle-jerk pseudotachylyte generation zones, both before and after melt generation. Finally, some field relationships suggest that lamproite magma and pseudotachylyte may have mixed in some generation zones, a possibility that is to be examined geochemically. The field relationships between pseudotachylyte faults and kimberlite dykes are not yet known. Piper (1981b, p.172) has described field relationships between kimberlite dykes and pseudotachylyte in this shear belt, but in the outcrops concerned lamproite rather than kimberlite dykes are exposed. Since dated kimberlites and lamproites from the Ikertôq Belt yield different ages (L.B. Smith, 1979), the dyke types should be clearly distinguished when field relationships with pseudotachylyte are described. Although lamproite dykes from elsewhere in the belt do yield an age of 1227 ± 12 Ma (L.R. Smith, 1979), the range of published ages for rocks of the West Greenland carbonatite-lamproite-kimberlite suite is so large (Larsen et al., 1983), that one hesitates to discriminate between the possible palaeomagnetic ages on this evidence.

The pseudotachylyte of this study lies along the contact between a biotite tonalitic gneiss and the pipe-like intrusion of the kimberlite-lamproite suite described by B.H. Scott (1981, pp. 5 and 18). The pseudotachylyte cuts the pipe, but is believed to have been generated in the tonalitic gneiss. Detailed descriptions of the pseudotachylytes at the northern boundary of the shear belt are given by Grocott (1977, 1981).

Description and mineralogy of structures

Amygdales, Outer Hebrides thrust

The pseudotachylyte veins, 3 cm in maximum thickness, have a plagioclase-microlitic texture

indicating primary crystallization from a silicate melt (Maddock, 1983). The veins contain approximately 20 modal % porphyroclasts of brittily deformed quartz and plagioclase. The amygdales vary from almost perfectly circular (believed spherical in 3D) to elliptical with increasing size over the range 20–200 μm maximum dimension. The larger elliptical examples are flattened parallel to the vein walls and have maximum aspect ratios of 2 (thin-section cut normal to vertical dip of vein). There is no evidence of microlite nucleation on the vesicle walls, but locally the microlite long axes are aligned parallel to the elongation of the vesicles. Segregation vesicles (R.E. Smith, 1967) were not observed. The modal proportion of amygdales is 3–5% and they are randomly distributed apart from being absent within 1 mm of the vein margin.

The mineralogy of the amygdales is shown in Table 1. Each amygdale contains 3–7 subhedral grains of one or more of the 'essential' phases (K-spar, quartz, sphene and epidote) which occupy most of the volume and exhibit quasi-drusy habit; the 'accessory' phases occupy the grain boundaries and inclusions within the essential phases (Plate I). Extreme modal mineralogical variation from one amygdale to another is considered *prima facie* evidence that they are indeed amygdales and not immiscible silicate liquid droplets (cf. Roedder, 1979, p. 44). In amygdales where quartz or alkali-feldspar dominate, sometimes to the total exclusion of all other phases [e.g. Plate I, (H)], substantial optical misorientation exists between the grains but there is no optical evidence of strain. Little chemical variation in essential or accessory phases exists within or between amygdales.

The accessory phases occur in varying proportions and restricted combinations; neither of the pairs actinolite and biotite or magnetite and sul-

PLATE I

Backscattered electron (BSE) micrographs and line drawings of amygdales in plagioclase microlitic pseudotachylyte from the OHT. *a*=actinolite; *b*=biotite; *e*=epidote; *f*=Fe-hydroxide; *k*=K-spar; *p*=pyrite (diagonal hachuring in F); *pl*=plagioclase; *q*=quartz; *s*=sphene. Scale in micrometers.

A and B. Typical amygdale showing sub-drusy habit of phases dominated by a large grain of epidote containing LREE-enriched epidote laths (lighter grey).

C and D. Amygdale with complex mineralogy; note the actinolite needle (*a*) which crosses grain boundaries between other phases.

E and F. Amygdale with mineralogy dominated by sphene and pyrite which is partially altered to Fe-hydroxide.

G. Amygdale containing sphene surrounding plagioclase (*pl*) believed to be a porphyroclast trapped during vesiculation.

H. Amygdale entirely filled by K-spar.

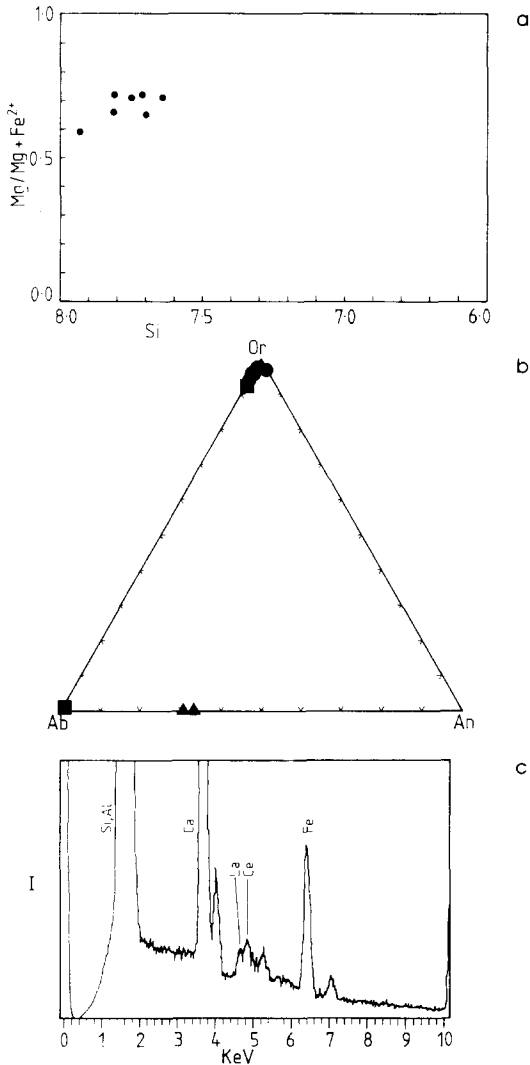


Fig. 1. Diagrams showing the compositions of selected phases in amygdales in Outer Hebrides Thrust pseudotachylytes.

a. Plot of Si vs. Mg/(Mg + Fe²⁺) formula units based on 23 (O) showing composition of acicular amphiboles [Fe²⁺ estimated by method of Papike et al. (1974)].

b. An-Ab-Or diagram (● = K-spar in amygdales; ▲ = (?) relict feldspar porphyroclast in amygdale; ■ = feldspars in microfractures).

c. Peak intensity (I) vs. energy (keV) plot showing qualitatively the presence of La and Ce in epidote 2 (lowest energy peaks only are annotated).

phide were observed coexisting in the same amygdale. Epidote 2 is found as laths (10 × 40 μm max) within epidote 1 [Plate I (A) and (B)], and contains up to 10 wt.% Ce₂O₃ and La₂O₃ – estimated from semi-quantitative analyses (Fig. 1c). Actinolite, perhaps the most abundant accessory phase,

occurs as needles (15 × 100 μm max.) which are included within the essential phases and cross their grain boundaries without deflection [Plate I, (C) and (D)]. This textural relationship implies growth of actinolite and subsequent inclusion within the other phases. The actinolite approaches end-member composition (Fig. 1a) containing very low Al₂O₃, Na₂O and K₂O. Laths and plates of biotite have an average composition shown in Table 1, but some of the grains are partially chloritized.

Pyrite, the most abundant opaque phase, sometimes achieves dimensions comparable to the essential phases [Plate I, (E) and (F)]. Magnetite occurs as small, rounded grains to 40 μm diameter. Both pyrite and magnetite are altered marginally and along grain boundaries to a brown/red Fe-hydroxide of bladed habit.

In one amygdale, a large angular grain of plagioclase of composition similar to the porphyroclasts (Fig. 1b) was found [Plate I, (G)]. The origin of this grain is uncertain; although it appears to contain inclusions of actinolite, it is probably a clast that was trapped during vesiculation.

The amygdale walls vary from sharp boundaries to narrow zones (< 10 μm wide) of replacement/alteration of the pseudotachylyte matrix by the phases within the amygdale proper.

The pseudotachylyte is cut by two generations of microfractures. The earliest microfractures (< 10 μm wide) appear to have been healed, mainly by K-spar, contemporaneously with the infilling of the amygdales. However, a minority of the amygdales are seen to be connected to microfractures. A later set of microfractures (up to 100 μm wide), demonstrably postdates the infilling of the amygdales and are healed by a xenoblastic intergrowth of albite and K-spar (Fig. 1b).

Porphyroclast replacement pseudomorphs, Outer Hebrides Thrust

Porphyroclast replacement pseudomorphs are distinguished from amygdales by their more irregular form and generally larger dimensions. In the amygdaloidal pseudotachylytes described above, incipient marginal alteration of the plagioclase porphyroclasts to epidote + clinozoisite + sericite + calcite has occurred especially adjacent to the microfractures. Similar marginal alteration of por-

phyroclasts has been noted by Philpotts (1964) (see Table 3).

In a more general sense, the pseudomorphs are best developed in pseudotachylytes with a high content of chlorite in their groundmass (probably devitrified glass) and with a high density of microfractures. An example (from a non-amygdaloidal pseudotachylyte) is shown in Plate II, (C) and (D). The plate shows a porphyroclast largely replaced by a rim of fibrous chlorite enclosing plates of weakly ferroan calcite, 200 μm across and with finely saw-toothed grain boundaries. Detailed examination in the SEM/microprobe reveals that the chlorite is replacing actinolitic hornblende and that the calcite includes small grains of quartz [Plate II, (D)]. The concentric pattern of replacement could result from nucleation effects or partial dissolution followed by void infilling, or both. Chlorite healed microfractures occur in close proximity to the replacement pseudomorph [Plate II, (C)].

Amygdales, Ikertôq Shear Belt

The 1.5 cm thick pseudotachylyte vein is conspicuously zoned. The central zone is brown and spherulitic with amygdales, the marginal zones are for the most part black and opaque and lack amygdales. The volume fraction of amygdales is 3–5%, and the lower figure is used in subsequent calculations. The amygdales, up to 1 mm long, show aspect ratios up to 10 or more, perhaps resulting from simple shear or flattening of the still hot and viscous pseudotachylyte.

The larger amygdales [Plate II, (A) and (B)] contain a zoned arrangement of chiefly carbonate minerals whose composition is given in Table 2. The pattern of zonation from amygdale centre to margin follows an increasingly complex mineralogy and decreasing grain size [Plate II, (B)]. The overall structure suggests vesicle infilling with nucleation dominating over growth initially (marginal zone) followed by growth dominating over nucleation (axial zone). Similar patterns, and indeed mineralogies, are frequently seen in vug and pore-space cementation and are explicable in terms of changing substrate structure and chemistry during crystallization. Growth of non-carbonate phases (barite, celadonite and magnetite) in the amygdales may have been relegated to grain boundary environments for similar reasons. The dolomite is presum-

ably secondary—perhaps after calcite, although no porosity increase is apparent. It is not clear whether the zoning in the dolomite [Plate II, (B)] is 'primary' (i.e. it formed during growth of the dolomite) or a later exsolution feature.

Celadonite, distinguished from glauconite by the former's negligible Al^{VI} content (Buckley et al., 1978), occurs as verdant wispy laths to $75 \times 15 \mu\text{m}$ maximum dimensions [Plate II (B)]. Celadonite is also found as an alteration product after biotite in the pseudotachylyte matrix and in the host-rock.

Carbonate- and barite-bearing microfractures intersect some of the amygdales with textures clearly demonstrating coeval filling of both structures [Plate II, (A) and (B)]. As with the Hebridean example however, by no means all of the amygdales are visibly connected to microfractures.

Discussion

Physical conditions of amygdale formation

In the Himalayan Langtang and Alpine Köfels landslides, frictionites with unequivocal vesicular texture are observed (Fig. 2; Scott and Drever, 1953; Erismann et al., 1977). The vesicles are testament to the exsolution of a vapour phase from the melt under conditions of low lithostatic pressure, estimated at 200 bar by Masch et al. (1985) for the Langtang slide. Amygdaloidal pseudotachylytes have been described from at least four other localities in addition to the Ikertôq Shear Belt and the Outer Hebrides Thrust (Table 3).

Determination of the physical conditions of vesicle/amygdale formation is of importance in attempts to specify the palaeoseismic source parameters of the earthquakes during which pseudotachylyte generation zones were formed (cf. Sibson, 1975; Grocott, 1981; J. Grocott and M. van Nes, in prep.). One significant source parameter is the drop in shearing stress in the plane of the fault during slip, and this parameter is limited during shallow earthquakes by the lithostatic pressure. If a method can be found whereby the formation depth of amygdaloidal pseudotachylyte can be estimated, the path would be open to more straightforward determination of palaeoseismic source parameters, and the search for scaling relationships between such source parameters could begin. In this section the

PLATE II

A



B

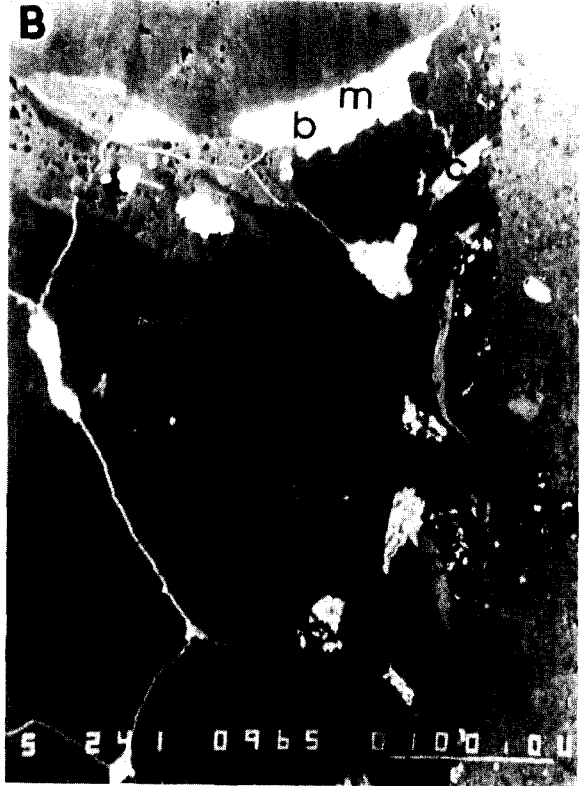


TABLE 2

Mineralogy of amygdales in Greenland pseudotachylyte

| Phase | Composition | Zonation/occurrence |
|--------------------------------------------------------|------------------------------------------------------------------------------------------------------------------------------------------------------------------------|--------------------------------------|
| Ferroan dolomite 1 Ferroan dolomite 2 | } Sid _{4.76} Magn _{43.60} Rhod _{1.06} Calc _{50.58} | } axial zone |
| Ferroan dolomite Ankerite | | |
| Barite Magnetite Celadonite Quartz Calcite | (K _{1.91} Ca _{0.06})(Mg _{1.58} Fe _{2.38} ³⁺)(Si _{7.90} Al _{0.02})O ₂₀ (OH) ₄ | } marginal zone and grain boundaries |
| | Sid _{1.31} Magn _{1.87} Rhod _{0.51} Calc _{96.31} | |



Fig. 2. BSE micrograph of highly vesicular landslide frictionite from Langtang, Himalayas. Scale bar = 50 μm .

possibilities for determining the depth of formation of pseudotachylyte using amygdales are reviewed, and a depth estimate is made for the Greenland pseudotachylyte described in detail in this paper.

In an unconfined igneous system it may be possible to estimate the depth of lava eruption on the sea floor if vesiculation has occurred (e.g. Moore, 1965, 1979). Bubbles form in the magma when the partial fictive vapour pressure of a dissolved gas phase exceeds the liquid pressure. They will only be preserved if this condition is maintained until the magma is largely solidified. In an unconfined body this can occur when the magma has access to the sea floor, and the liquid pressure is hydrostatic. The volume fraction of bubbles which form in a melt depends on the liquid pressure, temperature, the mass fraction of each gas phase and the solubility function of each gas phase (Macpherson, 1984).

Pseudotachylyte generation zones have no access to the surface and are thus confined systems. However, amygdaloidal pseudotachylyte is not uncommon (Table 3), and it is necessary to consider the circumstances in which the partial fictive vapour pressure of one or more of the gas phases could exceed the liquid pressure, at least transiently, in confined systems. Generation of pseudotachylyte on fault surfaces involves rapid, near-total, non-equi-

PLATE II

BSE micrographs of amygdale (Greenland) and porphyroclast replacement pseudomorph (OHT). Scale bar = 100 μm .

- A flattened vesicle with intersecting microfracture are infilled by large grains of carbonate with barite, celadonite and magnetite along grain boundaries.
- Detail of (A) showing irregularly zoned plates of ferroan dolomite (*d*) and grain boundary location of barite (*b*), celadonite (*c*) and magnetite (*m*). Note increase in grain size away from margin and continuity of microfracture and amygdale infilling.
- Porphyroclast replacement structure in chlorite-rich pseudotachylyte.; note proximity of chlorite healed microfracture (*m*).
- Detail of (C) showing zoned arrangement with rim of chlorite (*c*) enclosing calcite (*d*) with small grains of quartz.

TABLE 3

Literature-reported occurrences of amygdales in pseudotachylytes

| Reference | Locality | Description |
|-------------------|-----------------------------|-----------------------------------------------------------------------------------------------------------------------------------------------------------------------------------------------------------------------------------------------------------------------------------------------------------|
| Beckholmen (1982) | Sweden | irregular cavities to 3 mm dia. in spherulitic pseudotachylyte; filled with drusy quartz \pm calcite |
| Bisschoff (1962) | Vredefort (South Africa) | irregular/elliptical cavities parallel to flow-banding; filled with drusy calcite \pm quartz \pm chlorite \pm chalcopyrite |
| Nockolds (1944) | Antarctica | irregular/elliptical cavities filled with calcite + chlorite + epidote + quartz; microfractures healed with same phases may connect cavities |
| Philpotts (1964) | Canada | spherical/irregular cavities to 50 μ m dia., in microlitic pseudo-tachylyte; up to 20 modal vol.%; filled with quartz \pm calcite \pm magnetite \pm pyrite; infilling attributed to vapour precipitate from pseudotachylyte melt; rims of feldspar porphyroclasts locally replaced by carbonate |

librium melting [unpublished data of one of us (R.H.M.) suggest that a degree of selective melting can occur during pseudotachylyte genesis]. For rocks of tonalitic composition, melting will involve a volume increase of about 12% (Clark, 1966). Consequently a high liquid pressure will tend to develop in the melt on the fault surface, but is limited by the tensile strength of the surrounding rocks.

Veins of pseudotachylyte occur in three settings within pseudotachylyte generation zones; as lenses on non-planar generation surfaces, as veins which dilate pre-existing second order fractures and as injection veins (Grocott, 1981). Injection veins occupy simple extensional fractures and are commonly observed to have left planar pseudotachylyte generation surfaces at right angles. When melt is generated, liquid pressure (P_{liq}) may exceed lithostatic pressure (P_{lith}) due to volume change. (It is clear from field relationships that melt may continue to be generated on fault surfaces in spite of the expected reduction in friction.) If the differential stress is small, P_{liq} may approach a value of $-P_{lith} + \sigma_t$, where σ_t is the tensile strength (Fig. 3a). When extension failure occurs, P_{liq} will fall and it is assumed that vesiculation occurs at this stage in the injection vein. Preservation of bubbles is expected owing to rapid solidification of pseudotachylyte veins which are rarely wider than 1 or 2 cm.

In order to determine the depth of formation of amygdaloidal pseudotachylyte, data on the mass fraction of each gaseous component and their solubility functions are required. Solubility functions for H_2O in basalt and andesite at 1100°C have long been available (Hamilton et al., 1964), and more recently the solubility functions for CO_2 in basalt and andesite have been determined (Spera and Bergman, 1980; Harris, 1981). Macpherson (1984)

makes use of these data to predict the volumes of vesicles in submarine basalts, and his model may be used conditionally as a palaeodepth indicator if vesicle volume fractions are known. One problem with the method concerns the use of one solubility function for a wide range of basalt compositions, and there is certainly disagreement over the applicability of the results of Hamilton et al. (1964) to all andesite compositions (Sakuyama and Kushiro, 1979). The results of Hamilton et al. (1964) are difficult to apply to pseudotachylyte of andesitic composition formed at relatively shallow levels in the crust, because the solubility function for water in andesite is poorly defined at low pressures. Furthermore pseudotachylyte liquids may easily become superheated. On the other hand, Spera and Bergman (1980) show that the solubility of CO_2 is similar in both tholeiitic and andesitic melts at low pressures especially when the temperature exceeds 1450°C. In addition solubility of CO_2 is almost independent of temperature in andesitic magma at pressures below 4 kbar.

With these results and reservations in mind, the solubility functions for basalt may be applied to the pseudotachylytes of this study, noting that even at pressures below 1 kbar the solubility of water in andesite is not more than double that in basalt. Provided differences in the solubility function for CO_2 in andesite and basalt are indeed low under conditions relevant to amygdaloidal pseudotachylyte, use of basalt solubility data on the pseudotachylytes studied here should provide a depth estimate to within a factor of 2 or 3. This estimate will be improved as more solubility data becomes available.

The mass fraction of gaseous components originally in solution can be obtained from analysis of the country rocks of the pseudotachylyte since near-

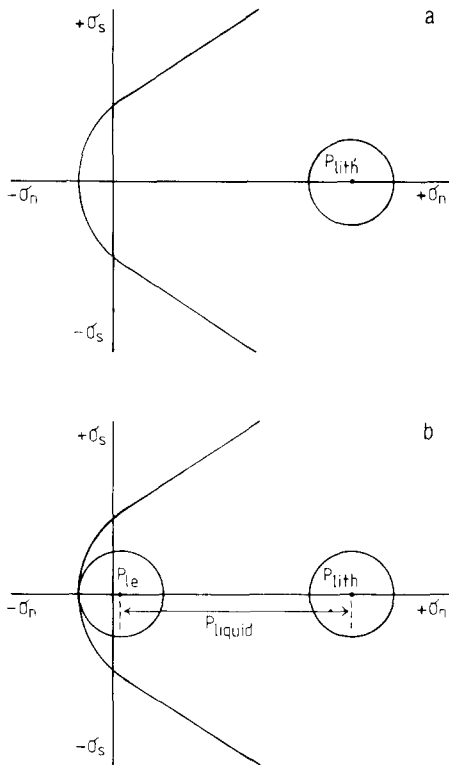


Fig. 3. a. Mohr diagram with a stress circle representing the state of stress in a pseudotachylyte generation zone at the stage of melt generation. The differential stress is low (a large fraction of the stress drop precedes melt generation (Grocott, 1981)), and a state of plane stress is assumed with lithostatic pressure equal to the mean stress.

b. Due to volume change on melting, pseudotachylyte is generated with a high fluid pressure. Pressure in the liquid will act against the lithostatic pressure. On the Mohr diagram this can be represented as a shift of the stress circle towards the origin. Extension failure occurs when the stress circle becomes tangent to the failure envelope. In the limit represented by a vanishingly small stress circle, the difference between the lithostatic pressure, P_{lith} , and the effective lithostatic pressure, P_{liq} , approaches a value of $-P_{lith} + \sigma_t$, where σ_t is the tensile strength. This is the maximum possible value of the liquid pressure. When fracturing occurs, liquid pressure is assumed to revert to lithostatic pressure, and under this condition the melt vesiculates.

total non-equilibrium melting was involved. In the Ikertôq Shear Belt the country rock temperature was below 250°C when most of the pseudotachylyte was generated (Grocott, 1977; Piper, 1981a), and there are no reasons to suppose that country rock compositions away from generation zones have changed since that time. Whole rock analyses of eight amphibolite facies tonalitic gneisses from the north

part of the shear belt have an average H₂O content of 0.38 wt.% (standard deviation 0.07) (Grocott, 1977, table 2-2b, p.100). Unfortunately CO₂ has not been determined for the same rocks, but other amphibolite facies gneisses of similar composition from the North Atlantic Shield yield rather consistent values in the range 0.1–0.2 wt.% CO₂ (e.g. Beach, 1976; Maddock, 1986b). There is no reason to expect significant departures from these values in the Greenland rocks, given the major element geochemical uniformity of such rocks in the shield.

The Greenland pseudotachylyte sample contains a minimum volume fraction of amygdaloids of 3%, and we assume that H₂O and CO₂ are the only vesicle forming components of importance (cf. Macpherson, 1984, p.73). Using a graph of volume % vesicles against pressure for 0.2 wt.% CO₂ and 0.5 wt.% H₂O (Macpherson, 1984, fig. 2), a lithostatic pressure of 410 bar is obtained corresponding to a depth of 1.6 km. In taking our lower estimate of amygdale volume (3%) and our higher estimate of CO₂ content of amphibolite facies tonalitic gneiss (0.2 wt.%), the result represents a maximum depth estimate.

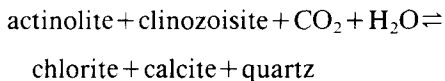
This result of course is only as good as the solubility functions used to obtain it and depends on the validity of the assumptions made to justify their use. Given solubility data truly applicable to pseudotachylytes, together with appropriate analyses for volatiles, more accurate determination of formation depths of amygdaloidal pseudotachylyte should be possible.

Allen (1979) has suggested that vesicles and (feldspar) microlites are mutually exclusive in pseudotachylytes and that both are related to depth of generation. This is demonstrably not the case in the present Hebridean example and in Canadian pseudotachylytes described by Philpotts (1964) (see Table 3). The presence or absence of microlites should not therefore be used to infer the depth of pseudotachylyte generation; their occurrence is more likely a function of host-rock/pseudotachylyte melt composition and crystal nucleation kinetics (Maddock, 1986b).

Significance of amygdale mineral assemblages

Leaving aside the Hebridean amygdaloidal pseudotachylytes, a marked mineralogical uniformity exists between the vein material in microfractures,

the replacement pseudomorphs, the Greenland pseudotachylyte amygdales and those described in the literature (Table 3). The widespread phase assemblage quartz \pm epidote \pm chlorite \pm carbonate indicates growth of these phases under conditions of low temperature and pressure – below those of greenschist facies metamorphism (Winkler, 1967). Notably, the common occurrence of carbonate suggests that cavity filling took place under conditions of moderate partial pressure of CO₂-favouring breakdown of Ca-silicates yielding calcite and an aluminous phase (especially chlorite). Microprobe analyses demonstrate chemical heterogeneity (i.e. disequilibrium) between, for example, chlorite in the replacement pseudomorph and the microfracture of Plate II, (C) and (D). For this reason it is difficult to write precise reactions describing the alteration/replacement/cavity filling processes. However, for the replacement pseudomorph described above an appropriate end-member reaction involving the phases present is (Deer et al., 1966):



with reaction tending to the r.h.s. favoured by moderate to high $P_{\text{H}_2\text{O}}$ and P_{CO_2} .

Summarizing, the mineralogy indicates that a low temperature ($\sim < 200^\circ\text{C}$) assemblage was precipitated from a hydrous fluid, locally or temporally enriched in CO₂ and containing solutes Si, Al, Ca, K, Fe, Mg and S. The timing of vesicle infilling and origin of the infilling fluids is difficult to ascertain. Philpotts (1964) suggested that pseudotachylyte amygdale minerals might be precipitated directly from vapour phases exsolved from the pseudotachylyte melt. This possibility seems unlikely in the present examples because of the mineralogy of the amygdales. Further, it is clear that in at least some cases vesicle infilling was related to healing of the microfractures [e.g. Plate II, (A) and (B)], and the sub-drusy habit is good evidence that the amygdales contain an assemblage precipitated in vesicle void space. In addition to the microfractures, the vesicles themselves may have locally provided a gross 'porosity' allowing ingress of fluids.

In contrast to the mineralogy discussed above, the mineralogy of the Hebridean pseudotachylyte amygdales indicates a higher temperature parage-

nesis comparable to that found in greenschist facies metavolcanics (e.g. Morrison, 1979; Studemeister, 1983). The assemblage (albite +) actinolite + epidote + quartz + sphene is indicative of greenschist facies conditions with $T \geq 350^\circ\text{C}$ and $P > 2$ kbar (Winkler, 1967). Further, the absence of carbonate suggests a low partial pressure of CO₂. The chemistry and mineralogy of these amygdales suggests that the phases were precipitated from a hydrous fluid enriched in Si, K, Ca, Ti, Al and Fe, with lesser amounts of Mg, S, P, Na, Ce and La. The LREE content of the epidote confirms that short range LREE mobility at least is possible in a hydrous fluid at low metamorphic grade (cf. Hellman et al., 1977; Nyström, 1984), and that the LREE's are preferentially partitioned into epidote rather than sphene. The minimal compositional variation between analyses of the same phase suggests that a reasonable degree of equilibrium was obtained. The extreme modal variation is perhaps due to different times of filling and kinetic nucleation effects.

As with the amygdales and filled cavities described above, this mineral assemblage appears to be restricted to structures with suitable mechanical pathways allowing fluid ingress. Thus the plagioclase microlites (An₂₅₋₄₀) and porphyroclasts (An₂₅) in the pseudotachylyte show no sign of albitization or adularization.

A problem arises with the Hebridean pseudotachylytes as to how vesicles, shown above to be likely to have formed at depths < 2 km, may contain a greenschist facies mineral assemblage implying $T \geq 350^\circ\text{C}$. A palaeogeothermal gradient of $175^\circ\text{C km}^{-1}$ is unlikely even in a potentially shear-heated thrust fault environment! An explanation for this may lie in the geological setting of these particular pseudotachylytes.

It was noted earlier that the sub-vertical quasi-conglomerate vein systems at Ruhba Ardvule, in which the amygdales occur, represent the earliest stages of pseudotachylyte generation, followed by E to W directed low angle thrusting. Sibson (1977b) has estimated a finite vertical component of thrust-sense movement across the main Outer Hebrides Thrust of 4.2 ± 2.1 km. Notwithstanding the sub-aerial erosion that must accompany thrusting, it is possible that the early amygdaloidal pseudotachylytes were buried by a substantial thrust pile, with higher PT conditions achieved through a combination of burial and shear-heating.

Conclusions

(1) The occurrence of amygdalites in pseudotachylytes from various localities strengthens the case for an origin by melting for these fault rocks (cf. Wenk, 1978; Masch et al., 1985).

(2) Using reasonable values for the H₂O and CO₂ contents of pseudotachylyte melt assumed to approximate andesite in composition, a depth of 1.6 km is estimated for the Greenland pseudotachylyte described in this paper.

(3) The carbonates and associated phases filling amygdalites in Greenland pseudotachylytes and other examples described in the literature, are consistent with vesicle infilling at shallow depths.

(4) Amygdalites are reported from Outer Hebrides Thrust pseudotachylytes for the first time.

(5) The greenschist facies mineral assemblage in Outer Hebrides Thrust pseudotachylyte amygdalites strongly suggests that the pseudotachylytes were buried to greater depths subsequent to their formation. This is consistent with field evidence and Sibson's (1977b) model for the thrust-sense movement of the Outer Hebrides Thrust.

(6) Structures superficially resembling amygdalites in pseudotachylytes are recognized as porphyroblast replacement pseudomorphs.

Acknowledgments

R.H.M. acknowledges the support of a NERC research studentship. Work on fault rocks in W. Greenland was supported by the Stichting Zuiver Wetenschappelyk Onderzoek (Z.W.O.) grant number 1811021 and the Stichting Dr. Schurmannfonds grant numbers 1983/01 and 1984/05. M.V.N. also acknowledges receipt of a Z.W.O. research studentship. SEM and electron microprobe work was performed at Imperial College. Silicate mineral analyses were recalculated using program SUPREC written by J.C. Rucklidge. We are grateful to Adrian Jones and two anonymous referees for their comments on an earlier draft of this paper.

References

- Allen, A.R., 1979. Mechanism of frictional fusion in fault zones. *J. Struct. Geol.*, 1: 231–243.
- Bak, J., Sørensen, K., Grocott, J., Korstgård, J.A., Nash, D. and Watterson, J., 1975. Tectonic implications of Precambrian shear belts in western Greenland. *Nature (London)*, 254: 567–569.
- Beach, A., 1976. The interrelations of fluid transport, deformation, geochemistry, and heat flow in early Proterozoic shear zones in the Lewisian complex. *Philos. Trans. R. Soc. London, Ser. A*, 280: 569–604.
- Beckholmen, M., 1982. Mylonites and pseudotachylytes associated with thrusting of the Köli Nappes, Tännforsfältet, central Swedish Caledonides. *Geol. Fören. Stockholm, Förh.*, 104: 23–32.
- Bischoff, A.A., 1962. The pseudotachylyte of the Vredefort Dome. *Trans. Geol. Soc. S. Afr.*, 65: 207–225.
- Buckley, H.A., Bevan, J.C., Brown, K.M. and Johnson, L.R., 1978. Glauconite and celadonite: two separate mineral species. *Mineral. Mag.*, 42: 373–382.
- Clark, S.P., 1966. Handbook of physical constants. *Geol. Soc. Am. Mem. No. 97*, 587 pp.
- Deer, W.A., Howie, R.A. and Zussman, J., 1966. An Introduction to the Rock-Forming Minerals. Longman, London, 528 pp.
- Erisman, Th., Heuberger, H. and Preuss, E., 1977. Das Bimmstein von Köfels (Tirol), ein Bergsturz-"frictionit". *Tschermaks Mineral. Petrogr. Mitt.*, 24: 67–119.
- Grocott, J., 1977. The northern boundary of the Ikertôq Shear Belt, West Greenland. Ph.D. Thesis, University of Liverpool, Liverpool (unpublished).
- Grocott, J., 1981. The fracture geometry of pseudotachylyte generation zones: a study of shear fractures formed during seismic events. *J. Struct. Geol.*, 3: 169–178.
- Hall, M.G. and Lloyd, G.E., 1981. The SEM examination of geological samples with a semiconductor backscattered electron detector. *Am. Mineral.*, 66: 362–368.
- Hamilton, D.L., Burnham, C.W. and Osborn, E.F., 1964. The solubility of water and effects of oxygen fugacity and water content on crystallization in mafic magmas. *J. Petrol.*, 5: 21–39.
- Harris, D.M., 1981. The concentration of CO₂ in submarine tholeiitic basalts. *J. Geol.*, 89: 689–701.
- Hellman, P.L., Smith, R.E. and Henderson, P., 1977. Rare earth element investigation of the Cliefdon Outcrop, N.S.W., Australia. *Contrib. Mineral. Petrol.*, 37: 91–109.
- Larsen, L.M., Rex, D.C. and Secher, K., 1983. The age of carbonatites, kimberlites and lamprophyres from southern West Greenland: recurrent alkaline magmatism during 2500 million years. *Lithos*, 16: 215–221.
- Macaudière, J., Brown, W.L. and Ohnenstetter, 1985. Microcrystalline textures resulting from rapid crystallization in a pseudotachylyte melt in a meta-anorthosite. *Contrib. Mineral. Petrol.*, 89: 39–51.
- Macpherson, G.J., 1984. A model for predicting the volumes of vesicles in submarine basalts. *J. Geol.*, 92: 73–82.
- Maddock, R.H., 1983. Melt origin of pseudotachylytes demonstrated by textures. *Geology*, 11: 105–108.
- Maddock, R.H., 1986a. Partial melting of lithic porphyroclasts in fault-generated pseudotachylytes. *Neues Jahrb., Mineral. Abh.*, 155: 1–14.
- Maddock, R.H., 1986b. The petrology and geological significance of some fault-generated pseudotachylytes. Ph.D. Thesis, University of London, London (unpublished).

- Masch, L., Wenk, H.R. and Preuss, E., 1985. Electron microscopy study of hyalomylonites – evidence for frictional melting in landslides. *Tectonophysics*, 115: 131–160.
- McKenzie, D. and Brune, J.N., 1972. Melting on fault planes during large earthquakes. *Geophys. J.R. Astron. Soc.*, 29: 65–79.
- Moore, J.G., 1965. Petrology of deep-sea basalt near Hawaii. *Am. J. Sci.*, 263: 40–52.
- Moore, J.G., 1979. Vesicularity and CO₂ in mid-ocean ridge basalt. *Nature (London)*, 282: 250–253.
- Morrison, M.A., 1979. Igneous and metamorphic geochemistry of Mull lavas. Ph.D. Thesis, University of London, London (unpublished).
- Nockolds, S.R., 1940. Petrology of rocks from Queen Mary Land. *Australas. Antarct. Exped.*, 1911–1914, *Sci. Rep.*, Ser. A, 4: 15–86.
- Nyström, J.O., 1984. Rare earth element mobility in vesicular lava during low grade metamorphism. *Contrib. Mineral. Petrol.*, 88: 328–331.
- Papike, J.L., Cameron, K.L. and Baldwin, K., 1974. Amphiboles and pyroxenes: characterization of other than quadrilateral components and estimates of ferric iron from microprobe data. *Geol. Soc. Am., Abstr. Prog.*, 6: 1053–1054.
- Passchier, C.W., 1982. Pseudotachylyte and the development of ultramylonite bands in the Saint-Barthelemy massif, French Pyrenees. *J. Struct. Geol.*, 4: 69–79.
- Philpotts, A.R., 1964. Origin of pseudotachylytes. *Am. J. Sci.*, 262: 1008–1035.
- Piper, J.A., 1981a. Palaeomagnetism of pseudotachylytes from the Ikertôq Shear Belt, and their relationship to the kimberlite-lamprophyre province, central-west Greenland. *Bull. Geol. Soc. Den.*, 30: 51–61.
- Piper, J.A., 1981b. Palaeomagnetic study of the (late Precambrian) West Greenland kimberlite-lamprophyre suite: definition of the Hadrynian Track. *Phys. Earth Planet. Inter.*, 27: 164–186.
- Roedder, E., 1979. Silicate liquid immiscibility in magmas. In: H.S. Yoder (Editor), *The Evolution of the Igneous Rocks*. Princeton University Press, Princeton, N.J., pp. 15–57.
- Sakuyama, M. and Kushiro, I., 1979. Vesiculation of hydrous andesitic melt and transport of alkalis by separated vapour phase. *Contrib. Mineral. Petrol.*, 71: 61–66.
- Scott, B.H., 1981. Kimberlite and lamproite dykes from Hölsteinborg, West Greenland. *Medd. Grönl. Geosci.*, No. 4, 24 pp.
- Scott, J.S. and Drever, H.I., 1953. Frictional fusion along a Himalayan thrust. *Proc. R. Soc. Edinburgh, Ser. B*, 65: 121–140.
- Sibson, R.H., 1975. Generation of pseudotachylyte by ancient seismic faulting. *Geophys. J.R. Astron. Soc.*, 43: 775–794.
- Sibson, R.H., 1977a. Fault rocks and fault mechanisms. *J. Geol. Soc.*, 133: 191–213.
- Sibson, R.H., 1977b. The Outer Hebrides Thrust: its structure, mechanism and deformation environment. Ph.D. Thesis, University of London, London (unpublished).
- Sibson, R.H., 1980. Transient discontinuities in ductile shear zones. *J. Struct. Geol.*, 2: 165–171.
- Smith, R.E., 1967. Segregation vesicles in basaltic lava. *Am. J. Sci.*, 265: 696–713.
- Smith, C.B., 1979. Rb–Sr mica ages of various kimberlites – Chairman's summaries and poster session abstracts, Kimberlite Symp. II, Cambridge, pp. 61–66.
- Smythe, D.K., Dobinson, A., McQuillin, R., Brewer, J.A., Matthews, D.H., Blundell, D.J. and Kelk, B., 1982. Deep structure of the Scottish Caledonides revealed by the MOIST reflection profile. *Nature (London)*, 299: 338–340.
- Spera, F.J. and Bergman, S.C., 1980. Carbon dioxide in igneous petrogenesis: I. Aspects of the dissolution of CO₂ in silicate liquids. *Contrib. Mineral. Petrol.*, 74: 55–66.
- Studemeister, P.A., 1983. The greenschist facies of an Archaean assemblage near Wawa, Ontario. *Can. J. Earth Sci.*, 20: 1409–1420.
- Watterson, J., 1975. Mechanism for persistence of tectonic lineaments. *Nature (London)*, 253: 520–522.
- Wenk, H.R., 1978. Are pseudotachylytes products of fracture or fusion? *Geology*, 6: 507–511.
- Winkler, H.G.F., 1967. *Petrogenesis of Metamorphic Rocks*. Springer, New York, N.Y., 237 pp.